July 2018

Experimental Verification of Indirect Evaporative Cooling-Assisted Internally Cooled Liquid Desiccant Dehumidifier

Joon-young Park
Hanyang university, Korea, Republic of (South Korea), jego2000@hanyang.ac.kr

Jae-Weon Jeong
Hanyang university, Korea, Republic of (South Korea), jjwarc@hanyang.ac.kr

Experimental verification of indirect evaporative cooling assisted internally cooled liquid desiccant dehumidifier

Joon-Young PARK, Jae-Weon JEONG*

Hanyang University, Department of Architectural Engineering, Seoul, Republic of Korea

jjwarc@hanyang.ac.kr

* Corresponding Author

ABSTRACT

The main objective of this study is to estimate the system performance of an evaporative cooling assisted internally cooled liquid desiccant dehumidifier (ICLD). The feasibility of an evaporative cooling assisted ICLD is analyzed using an environmental climate chamber test for a variation in the working airflow on the evaporative cooling channel. In the process air channel of the ICLD, the air stream was maintained at a constant mass flow rate when the working air steam was changed to modulate the increase in airflow ratio from 0.25 to 1.0. The ICLD performance was measured under a constant temperature and humidity to simulate hot and humid outdoor air conditions. To evaluate its performance, the cooling capacity, wet-bulb effectiveness, coefficient of performance, and volumetric mass transfer coefficient of the ICLD were evaluated based on the measured data. As the results indicate, the 0.5 ratio of airflow between the working and process air stream showed a higher performance in terms of dehumidification and sensible cooling than a different airflow ratio.

1. INTRODUCTION

During a hot and humid cooling season, air conditioning systems require the removal of the latent heat from buildings and outdoor air during the air conditioning. Therefore, to control the latent load, a well-adapted air-conditioning system is necessary. Liquid desiccant (LD) cooling technology has been drawing interest as an alternative to conventional vapor-compression heating, ventilation, and air conditioning systems when using low-grade heating (i.e., 60–80 ℃), such as with geothermal, solar, and waste heat (Goetzler et al., 2014).

The moisture removal of the induced outdoor air is achieved using an LD unit operation, and the process air is then cooled using an additional cooling device such as an evaporative cooler (Kim et al., 2013; Dieckmann et al., 2004). For the last couple of decades, many researchers have focused on the understanding and numerical or empirical modeling of the dehumidification process in LD systems, particularly in a packed bed dehumidifier (Chung and Luo, 1999; Martin and Goswami, 2000; Liu et al., 2006, 2011 (1), (2); Park et al., 2016).

Normally, a packed bed dehumidifier can provide a better deep heat and mass transfer performance compared with other dehumidifier technologies, and uses an adiabatic dehumidification process without any additional heat transfer in the dehumidifier. While processing the dehumidification, an exothermic reaction occurs. Therefore, cooling sources are required to control the exothermic reaction during the dehumidification process. If cooling sources are not supplied, the desiccant solution temperature increases with the dehumidification process, leading to a decrease in the dehumidification capacity of the packed bed dehumidifier (Gao et al., 2013). Therefore, the temperature of the dehumidifier should be adjusted to maintain the dehumidification performance.

Many researchers have focused on the potential of an internally cooled liquid desiccant dehumidifier (ICLD) to improve the heat and mass transfer between the desiccant solution and processed air. Gao et al. (2013) proposed a partial ICLD to evaluate between the adiabatic and ICLD performance. Based on the adjustment methods for the cooling source supply, both systems are analyzed to compare the dehumidification performance. They found that the

ICLD has a merit in terms of the dehumidification performance under a lower temperature and the concentration of the inlet desiccant solution in the dehumidifier. Lowenstein et al. (2007) suggested a low solution mass flow ICLD that consists of a plastic plate heat exchanger to maintain a low liquid-to-gas ratio compared to a conventional LD system. In the heat exchanger, chilled water is used to prevent heat transfer from the exothermic reaction of the dehumidification to the process air stream.

Qi et al. (2013) proposed a prediction model for an internally cooled and heated LD system. This prediction model can define three types of effectiveness of an internally cooled and heated LD system: enthalpy, moisture, and temperature effectiveness. In addition, the system outlet parameters of all fluids including the air, desiccant solution, and heating or cooling fluid can be calculated accurately under different operating conditions. Zhang et al. (2013) examined an ICLD dehumidifier using a fin and tube heat exchanger. They analyzed the performance of the ICLD dehumidifier using performance indicators, namely, the moisture removal rate, dehumidification effectiveness, and volume mass transfer coefficient, to evaluate the system performance. Based on the results of this study, the experimental data agree well with previous studies and a numerical model with an error bound of 20%.

Kessling et al. (1998) investigated an ICLD integrated with a solar energy application. The exothermic reaction between the desiccant solution and air was analyzed through a comparison of the adiabatic and ICLD performance. To increase the dehumidification performance of an LD system, each channel of the dehumidifier was designed to supply chilled water to prevent an increase in temperature. Yin et al. (2008) proposed a new type of internally cooled and heated LD system using a plate fin heat exchanger. They evaluated the cooling performance of the ICLD based on the temperature of the inlet desiccant solution. In addition, according to the measurements of the ICLD performance, the dehumidification cooling performance of the ICLD was compared with an adiabatic LD system to verify the measured data.

Consequently, the purpose of this study is to investigate empirically the performance of an ICLD using evaporative cooling for use of internal cooling sources. The ICLD used in this study was designed for a cross-flow type between the process and working air streams. The impact of the variation in working air stream on the dehumidification cooling performance of an ICLD is a key factor of this study. Therefore, the dehumidification cooling performance of an ICLD was examined under various working airflows in an environmental climate chamber. The airflow ratio (AFR) between the working and process air was adjusted from 0.25 to 1.0 while increasing the AFR 0.25 for each experimental step. The measured data were estimated using system performance indicators such as the cooling capacity, wet-bulb effectiveness, volume mass transfer coefficient, and coefficient of performance (COP) of the ICLD.

2. EXPERIMENT SETUP

The cross-flow ICLD was selected to examine the performance of the dehumidification and sensible cooling. The ICLD applied in this work uses a 38.2% lithium chloride (LiCl) solution to dehumidify the process air. The configuration of the ICLD shown in Figure 1 was designed to modulate the internal cooling effect using evaporative cooling in the working air channel of the ICLD. In the process air channel of the ICLD, the air stream and liquid desiccant solution pass through the process air channel of the ICLD in a parallel path. When the air stream passes through the channel, it is sensibly cooled and dehumidified by the liquid desiccant solution. Meanwhile, in the working air channel of the ICLD, evaporative cooling is applied to control the exothermic reaction of the dehumidification in the process air channel of the ICLD, and to cool the process air stream through a heat transfer from its evaporative cooling.

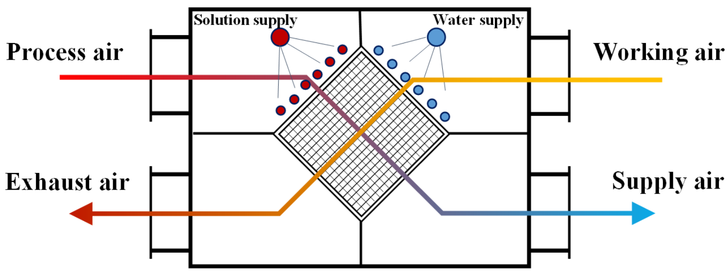

Figure 1. Configuration of the evaporative cooling assisted internally cooled liquid desiccant dehumidifier.

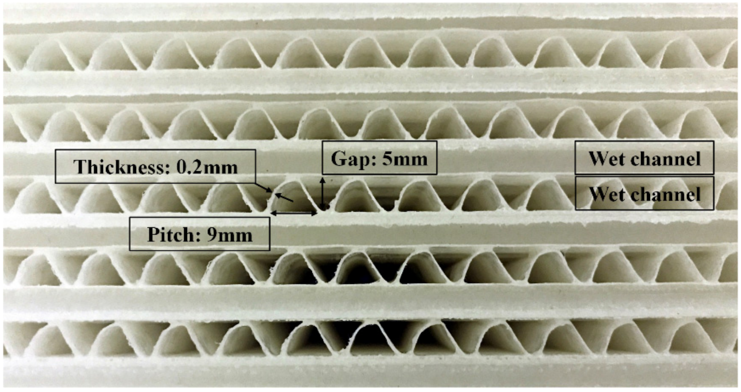

Figure 2. Geometry of the ICLD.

The ICLD consists of 30 pairs of wet channels in the process and working air, respectively. The wet channels are configured out of corrugated fiber fabricated using sheets of polyethylene phthalate and paper. The process and working air channel are supplied with a liquid desiccant solution and water uniformly on the wet channel surface. The geometry of the wet channel is shown in Figure 2. The thickness of the channel is 0.2 mm, and the gap between each channel is 5 mm with a 9 mm channel pitch. When the ICLD volume is 0.099 m3, the height of the ICLD is 340 mm, and length and width are both 540 mm. Table 1 shows the dimensions of the ICLD used in the experiments.

Table 1. Detained dimensions of the wet channel in the ICLD.

Wet channel gap	5 mm
Wet channel pitch	9 mm
Wet channel thickness	0.2 mm
ICLD unit length	540 mm
ICLD unit width	540 mm
ICLD unit height	340 mm

3. PERFORMANCE MEASUREMENT

3.1 Measurement equipment

To evaluate the dehumidification cooling performance of the ICLD operation, the ICLD unit was placed in environmental climate chambers (Figure 3). The environmental climate chambers were under two different conditions to simulate the outdoor and room conditions, respectively. Each chamber was adjusted using constant temperature and humidity levels to meet the target experimental conditions. The outdoor air chamber was controlled to modify the hot and humid conditions; meanwhile, the room air chamber maintained general room conditions to apply the evaporative cooling of the working air.

In each chamber, an environment control unit was installed to maintain the target experimental conditions. The environment control unit has a cooling capacity of 12.55 kW and a heating capacity of 5 kW, with a controlled air distribution of 2500 m3/h. The dry-bulb and wet-bulb temperatures of the ICLD inlet and outlet were measured using resistance thermometer detectors (i.e., RTDs) located in the code testers. The humidity ratio of the process and working air stream was calculated based on the measured values of the dry- and wet-bulb temperatures. The mass flow rate of each air stream was determined based on the pressure drops measured using differential pressure sensors and static pressure sensors in each code tester. The temperatures of the inlet desiccant solution in the process channel and the inlet water in working channel were measured using a thermocouple. The liquid desiccant solution concentration was measured using a glass hydrometer at the inlet and outlet concentrations, respectively. Table 2 lists the range and accuracy of each piece of measurement equipment, and Figure 4 shows the measurement setup used to evaluate the performance of the ICLD.

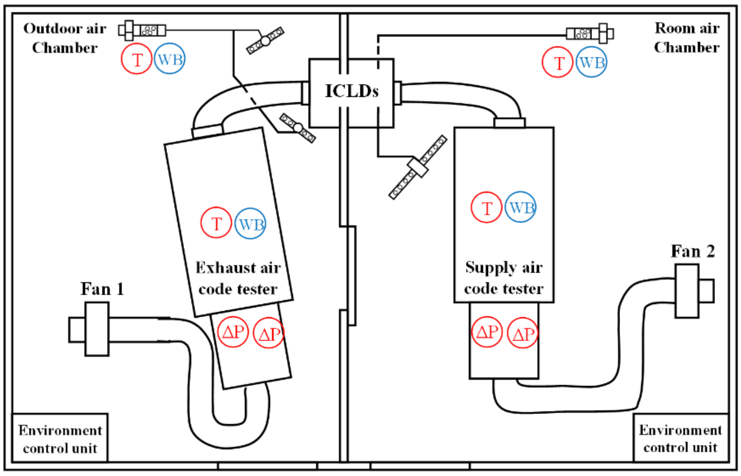

Figure 3. Schematic diagram of the environmental climate chambers.

Table 2. Characteristics of the measurement devices.

Device	Type	Range	Accuracy
Dry-bulb Temperature	RTD sensor	-50°C to 150°C	± (0.15 +0.002t) °C
Wet-bulb Temperature	RTD sensor	-60°C to 260°C	± (0.15 +0.002t) °C
Air flow	Differential pressure sensor	0 – 1250 Pa	± 0.3%
Static pressure	Differential pressure sensor	0 – 1000 Pa	± 0.3%
Temperature Sensor	Thermocouple	-80°C to 300°C	± (0.05 +0.005t) °C
Density meter	Glass hydrometer	1.0 – 1.5 g/ml	0.001 g/ml

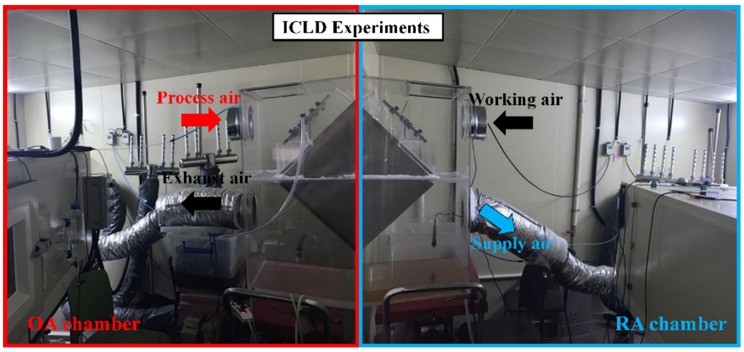

Figure 4. Experimental setup of ICLD.

3.2 Experimental overview

To evaluate the performance of the ICLD under different working airflow rates, an experiment was conducted to estimate the dehumidification cooling of the process air. The process air stream was maintained at a constant mass flow rate of 0.167 kg/s (i.e., 500 m3/h), and the working air was changed to modulate the AFR, which increased from 0.25 to 1.0 (Table 3).

Table 3. Experimental conditions in the ICLD.

No.	**Process air mass flow ($\dot{m}_{PA}$)**	**Working air mass flow ($\dot{m}_{WA}$)**	**AFR ($\dot{m}_{WA}/\dot{m}_{PA}$)**
1	0.167 kg/s	0.04 kg/s	0.25
2	0.167 kg/s	0.08 kg/s	0.5
3	0.167 kg/s	0.12 kg/s	0.75
4	0.167 kg/s	0.167 kg/s	1.0

Based on the experimental setup, when the working air mass flow varied, the mass flow of the process air was fixed to allow only the change in the performance of the ICLD to be evaluated according to the variation in mass flow of the working air. The inlet condition of the process air was controlled by the outdoor air chamber, which was set to a dry-bulb temperature of 32 ℃ and 40% relative humidity (i.e., 11.96 g/kg) for modulating the hot and humid conditions of outdoor air. To adjust the working air conditions, the room air chamber was maintained at a dry-bulb temperature of 24 ℃ and 60% relative humidity (i.e., wet-bulb temperature of 18.6 ℃), based on the ASHRAE Standard 55 (2013).

In addition, in the process air channel, the temperature of the inlet liquid desiccant solution was supplied at 24 ℃, with a mass flow rate of 0.02 kg/s using the solution distributor. For the concentration of the aqueous LiCl solution, about a 38% aqueous solution was applied during all experiments. Meanwhile, in the working air channel, the water was supplied at 22 ℃, with a 0.02 kg/s mass flow rate, which was the same value compared with mass flow rate of the solution used for generating the evaporative cooling.

3.3 Uncertainty analysis

The overall uncertainty of the experimental data was determined based on the ASHRAE guidelines (2010). To estimate the uncertainty value, using both basis (b_x) and precision (p_x) uncertainty calculated for the measured value at inlet and outlet of ICLD system (X_i). The uncertainty analysis was carried out via the Engineering Equation Solver (EES), a commercial equation solver (Klein 2004) and it was indicated in the experimental results. The overall uncertainty of the experimental data was determined based on the ASHRAE guidelines (2010).

$$U_x = (\mathrm{b}_x^2 + p_x^2)^{1/2} \tag{1}$$

$$\mathrm{b}_x = \left[\sum_{i=1}^{n}\left(\frac{\partial x}{\partial x_i} b_{x_i}\right)^2\right]^{1/2} \tag{2}$$

$$p_x = \frac{2S_r}{\sqrt{M}} \tag{3}$$

3.4 Performance index

The dehumidification cooling performance of the ICLD was evaluated using performance indicators such as the cooling capacity, wet-bulb effectiveness, volumetric mass transfer coefficient, and the coefficient of performance (i.e., COP). To estimate the dehumidification cooling performance of the ICLD, the cooling capacity and wet-bulb effectiveness are used to estimate the evaporative cooling of the process air, and the volumetric mass transfer coefficient is applied to estimate the dehumidification of the process air (Zhang et al., 2013; Kim et al., 2017). The cooling capacity and effectiveness of the wet-bulb were determined using Equations (4) and (5). In Equations (4), and indicate the enthalpy of the process air at the inlet and outlet of the process air channel, respectively, and represents the mass flow rate of the process air. Meanwhile, in Equation (5), and represent the temperature of process air at the inlet and outlet of the process air channel, and represents the wet-bulb temperature of the working air at the inlet of the working air channel.

$$C = \dot{m}_{PA}\,(h_{PA,in} - h_{PA,out}) \tag{4}$$

$$\varepsilon_{wet} = \frac{(T_{PA,in} - T_{PA,out})}{(T_{PA,in} - WBT_{WA,in})} \tag{5}$$

To evaluate the dehumidification performance of the ICLD, the moisture removal rate can be estimated using Equation (6), and the volumetric mass transfer coefficient is calculated using Equation (7). These equations are commonly used to estimate the dehumidification performance of a liquid desiccant unit. In Equation (6), and represent the humidity ratio of the process air at the inlet and outlet of the process air channel, respectively. In addition, in Equation (7), and represent the volume of the ICLD and the equilibrium humidity ratio of the inlet desiccant solution, respectively.

$$m_w = \dot{m}_{PA}\,(\omega_{PA,in} - \omega_{PA,out}) \tag{6}$$

$$K_v = \frac{m_w}{V\,(\omega_{PA,in} - \omega_{e,sol})} \tag{7}$$

In addition, based on the cooling capacity of the ICLD (Equation 4), the COP of the ICLD was estimated using Equation (8). In Equation (8), represents the overall electrical energy consumption of the ICLD including the fan and pump energy in both the process and working air channels used in the experiments.

$$COP = \frac{Cooling\ capacity}{E} = \frac{\dot{m}_{PA}(h_{PA,in} - h_{PA,out})}{\Sigma E_{fan} + \Sigma E_{pump}} \tag{8}$$

4. EXPERIMENTAL RESULTS

To evaluate the impact of the working airflow variation on the performance of the ICLD, the experimental data were applied when the ICDL was operated in the environmental climate chamber. The ICLD performance was measured under a constant temperature and humidity, which simulated hot and humid outdoor air conditions (i.e., 32 °C, 11.96 g/kg). The mass flow rate of the process air stream was maintained at a constant, when the mass flow rate of the working air steam was changed to modulate the AFR increase from 0.25 to 1.0.

4.1 Results

Based on the sequence of experiments (Table 3), the dehumidification cooling performance of the ICLD was measured, the results of which, as summarized in Table 4, were converted into the average values. While examining the measured experimental data, the desiccant solution and water were adjusted at a constant mass flow of 0.02 kg/s, and the temperatures of the inlet desiccant solution and water were maintained at 23 °C and 21 °C, respectively. In addition, the concentration of the LiCl solution was 38.2% for all experiments.

Table 4. Measured average data value of the ICLD

No	$\dot{m}_{PA}$ [kg/s]	$\dot{m}_{WA}$ [kg/s]	$T_{PA,in}$ [°C]	$\omega_{PA,in}$ [g/kg]	$WBT_{WA,in}$ [°C]	$T_{PA,out}$ [°C]	$\omega_{PA,out}$ [g/kg]	C [kW]	ε_{wet} [-]	K_v [kg/m^{3}s]
1	0.167±0.02	0.04±0.01	32.4±0.2	12.3±0.1	18.4±0.3	27.4±0.4	11.7±0.1	1.09±0.3	0.36±0.1	0.13±0.1
2	0.167±0.03	0.08±0.02	32.3±0.2	12.0±0.1	19.1±0.3	25.8±0.3	10.3±0.1	1.82±0.2	0.49±0.1	0.43±0.1
3	0.167±0.02	0.12±0.01	32.3±0.3	12.2±.0.1	18.7±0.2	25.7±0.2	11.2±0.2	1.36±0.2	0.45±0.1	0.25±0.1
4	0.167±0.02	0.167±0.03	31.9±0.3	11.9±0.1	19.5±0.4	27.4±0.4	10.8±0.1	1.12±0.1	0.35±0.1	0.26±0.1

Figure 5 shows the cooling capacity of the ICLD measured under various working airflows. It can be seen that the AFR between the working and process air streams was 0.5, which is higher than the other AFR values, and that the cooling capacity was decreased when the working airflow was lower or higher than the AFR of 0.5.

As shown in Figure 6, the highest wet-bulb effectiveness was exhibited at an AFR of 0.5 between the working and process air streams. Normally, according to a previous study on an indirect evaporative cooler (Velasco et al., 2012; Tejero et al., 2013), the wet-bulb effectiveness decreased when the airflow rate increased in the process and working air channels. However, the experiments of the ICLD showed that the maximum effectiveness of the wet-bulb was obtained at a critical AFR of 0.5. In addition, owing to the decrease in the effectiveness of the wet-bulb, the process air temperature when leaving the ICLD was increased.

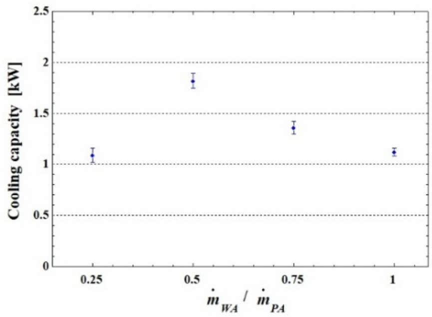

Figure 5. Cooling capacity of ICLD on the various working air flow.

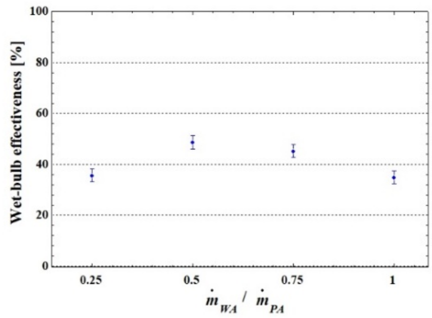

Figure 6. Wet-bulb effectiveness of ICLD on the various working air flow.

Figure 7 shows the volumetric mass transfer coefficient of the ICLD used in this study, which was indicated to be from 0.13 to 0.43 according to the variation in working airflow. It can be seen that the AFR of 0.5 was higher than the other values. The process air mass flow was adjusted using a constant value in all experiment setups, and thus the difference in volumetric mass transfer coefficient was determined through the moisture removal of each experiment. Therefore, it was confirmed that the dehumidification of the process air was the highest when the AFR was 0.5. In addition, as shown in Table 5, the volumetric mass transfer coefficient measured in this study showed a similar value as in previous studies on ICLDs (Lowenstein et al., 2007; Kessling et al., 1998; Yin et al., 2008).

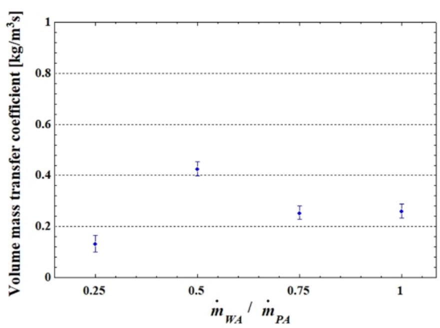

Figure 7. Volume mass transfer coefficient of ICLD on the various working air flow

Table 5. Comparison of the experimental data of ICLD

Ref.	Desiccant Solution	$\frac{\dot{m}_{sol}}{\dot{m}_{PA}}$	$\frac{\dot{m}_{sol}}{\dot{m}_{water}}$	$X_{sol,in}$ [%]	T_{water} [°C]	K_V [kg/m^{3}s]
Lowenstein et al. (2007)	LiCl	0.08 – 2	0.06 – 2	43.0	18.3 – 29.4	7.8 – 12.1
Kessling et al. (1998)	LiCl	0.01 – 0.1	0.06 – 0.25	40.2	24	0.12 – 0.17
Yin et al. (2008)	LiCl	1.1 – 2	0.68 – 0.71	37.7 - 38.8	19.5 – 24.5	0.9 – 1.9
Present study	LiCl	0.12	1	38.2	21	0.13 – 0.43

Figure 8 shows the overall coefficient of performance of the ICLD used in this study, which was indicated to be from 6.97 to 13.94, which varied based on the difference in working airflow. It can be seen that the AFR of 0.5 resulted in the highest COP value, i.e., 13.94, owing to the relatively high cooling capacity and low electric energy consumption. In these experiments, 40 W capacity pumps were used to maintain a constant mass flow rate of both the desiccant solution and water, and thus the pressure drops in the process and working air channels did not show a significant difference. Thus, the overall COP value depended on the cooling capacity of the ICLD, and showed similar patterns in the results of the cooling capacity.

4.2 Discussion

As with the results from the previous section, the four system performance indicators were analyzed based on the AFR between the working air and process air streams (e.g., 0.25, 0.5, 0.75, and 1.0). In terms of the impact of the AFR, the value of 0.5 between the working air and process air was better than the other AFR values. This tendency is similar with that of the wet-bulb effectiveness and the volume mass transfer coefficient exhibited by the ICLD operation described in this study.

During the experiment, the wet-bulb temperature of the inlet working air of the ICLD showed a similar value for each experimental step. In addition, the temperature and mass flow of the water supply were also equally modulated. Only the working airflow rate was tested to determine its effect on the performance of the ICLD. As shown in previous research, the channel gap significantly impacts the evaporative cooling performance (Chen et al., 2016 (1), (2)); in addition, a balanced AFR is important to maintain the evaporative cooling performance (Kim et al., 2017). However, in this experiment, the channel gap was fixed to 0.5 mm, and the AFR was changed from 0.25 to 1.0 to modify its impact on the evaporative cooling in the working air channel.

In addition, the impact of the AFR affected the dehumidification performance of the ICLD. In previous research, an AFR of 0.7 to 0.9 exhibited an upper limit on the AFR of the ICLD (Saman and Alizsdeh, 2001). Similarly, the results of this study showed that the AFR values of 0.5 to 0.75 were higher than in a balanced flow. It can be determined that the total load removed in the process air channel is determined by the available capacity of evaporative cooling in the working air channel. In this study, the geometry, flow type, and channel of the ICLD impacted the dehumidification cooling performance of the ICLD. When the AFR value was 0.5, the dehumidification cooling performance of the ICLD was found to be the highest. Thus, the working airflow rate does not need to be balanced with the process air stream to conduct dehumidification cooling while maintaining the energy consumption of the system.

5. CONCULSIONS

In this research, the impact of the variation in working airflow on an evaporative cooling assisted ICLD was evaluated. The dehumidification cooling performance of the ICLD was examined in an environmental climate chamber while changing the working airflow rate. The AFR between the working and process air was adjusted from 0.25 to 1.0 at increments of 0.25 for each experimental step. The experimental data were estimated based upon the performance parameters, such as the cooling capacity, wet-bulb effectiveness, volume mass transfer coefficient, and COP. According to the measured data, an AFR of 0.5 resulted in a significantly higher performance of the ICLD than the other AFR values.

Furthermore, the experimental results indicate that an AFR of 0.5 can achieve a higher dehumidification than the other AFR values. This tendency can be explained based on the characteristics of the geometry and contact flow type of ICLD used. Based on previous research on evaporative cooling, the channel gap and contact flow type had an impact on the cooling performance of the evaporative cooling. In addition, the ICLD exhibited a lower dehumidification performance than that of the adiabatic LD dehumidifier. However, considering the enthalpy change of the process air, it is considered to be a more effective method for dehumidification cooling of the process air. The AFR value of 0.5 confirmed in this study can be judged based on the upper limit of the working air and the process air, and is significant as the upper limit of the ICLD used in this study, as compared with an AFR value of 0.7 to 0.9, which was confirmed in previous research.

NOMENCLATURE

b	bias standard uncertainty	
C	cooling capacity	(kW)
COP	coefficient of performance	
E	energy consumption	
h	enthalpy	(kJ/kg)
K	volume mass transfer coefficient	(kg/m^{3}s)
M	number of multiple tests	
m	moisture removal rate	(kg/s)
$\dot{m}$	mass flow rate	(kg/s)
p	precision standard uncertainty	
s_r	standard deviation of result	
T	temperature	(°C)
U	overall uncertainty	
V	volume	(m^3)
WBT	wet-bulb temperature	(°C)
ε	effectiveness	(-)
ω	humidity ratio	(kg/kg)

Subscript

e	equilibrium
in	inlet
out	outlet
PA	process air
sol	desiccant solution
v	volume
w	moisture
WA	working air
wet	wet-bulb

REFERENCES

Goetzler, W., Zogg, R., Young, J., and Johnson, C. (2014). Energy Savings Potential and RD&D Opportunities for Non-Vapor-Compression HVAC Technologies. *Navigant Consulting Inc.,* prepared for US Department of Energy.

Kim M.-H., Park J.-S., and Jeong, J.-W. (2013) “Energy saving potential of liquid desiccant in evaporative-cooling-assisted 100% outdoor air system”, *Energy*, Vol. 59, pp. 726–736.

Dieckmann, J., Roth, K. W., and Brodrick, J. (2004). “Liquid desiccant air conditioners,” *ASHRAE journal*, Vol. 46 (4), pp. 58-59.

Tsair-Wang Chung, Chung-Ming Luo. (1999) "Vapor Pressures of the Aqueous Desiccant", *Journal of Chemical and Engineering Data*, Vol. 44, pp. 1024-1027.

Viktoria Martin, D. Yogi Goswami. (2000) "Effectiveness of heat and mass transfer processes in packed bed liquid desiccant dehumidifier/regenerator", *HVAC&R Research*, Vol. 6, No. 1, pp. 21-39.

X.H. Liu, K.Y. Qu, Y. Jiang. (2006) "Empirical correlations to predict the performance of the dehumidifier using liquid desiccant in heat and mass transfer", *Renewable Energy*, Vol. 31, pp. 1627-1639.
X.H. Liu, X.Q. Yi, Y. Jiang. (2011) "Mass transfer performance comparison of two commonly used liquid desiccants: LiBr and LiCl aqueous solution", *Energy Conversion and management*, Vol. 52, pp. 180-190.
X.H. Liu, Y. Zhang, K.Y. Qu, Y. Jiang. (2011) "Experimental study on mass transfer performances of cross dehumidifier using liquid desiccant", *Energy Conversion and management*, Vol. 47, pp. 2682-2692.
Park J.-Y., Yoon D.-S., Lee S.-J., and Jeong, J.-W. (2016) "Empirical model for predicting the dehumidification effectiveness of a liquid desiccant system", *Energy and buildings*, Vol. 126 pp. 447–454.
Gao W. Z., Shi Y. R., Cheng Y. P., and Sun W. Z. (2013) "Experimental study on partially internally cooled dehumidification in liquid desiccant air conditioning system", *Energy and Buildings*, Vol. 61, pp. 202–209.
Lowenstein A., Slayzak S., and Kozubal E. "A zero carryover liquid-desiccant air conditioner for solar applications" In: *Proceedings of the ASME international solar energy conference*; 2007. pp. 397-407.
Qi R., Lu L., and Yang H. (2013) "Development of simplified prediction model for internally cooled/heated liquid desiccant dehumidification system", *Energy and Buildings*, Vol. 59, pp. 133-142.
Zhang T., Liu X., Jiang J., Chang X., and Jiang Y. (2103) "Experimental analysis of an internally-cooled liquid desiccant dehumidifier", *Building and Environment*, Vol. 63, pp. 1-10.
Kessling W., Laevemann E., and Kapfhammer C. (1998) "Energy storage for desiccant cooling systems component development", *Solar energy*, Vol. 64, pp. 209-221.
Yin Y., Zhang X., Wang G., and Luo L. (2008) "Experimental study on a new internally cooled/heated dehumidifier/regenerator of liquid desiccant systems", *International Journal of Refrigeration*, Vol. 31, pp. 857-866.
ASHRAE (2013). ANSI/ASHRAE/IES Standard 55. Thermal environmental conditions for human occupancy. *American Society of Heating, Refrigerating and Air-Conditioning Engineers*, Inc.
ASHRAE (2010). ASHRAE Guideline 2. Engineering Analysis of Experimental Data. *American Society of Heating, Refrigerating and Air-Conditioning Engineers*, Inc.
Klein S.A. F-Chart Software, Engineering Equation Solver, EES Manual, Chapter 1: Getting started. Solar Energy Laboratory, *University of Wisconsin-Madison*, (2004) 2013.
Kim H-J., Ham S-W., Yoon D-S., and Jeong J-W. (2017) "Cooling performance measurement of two cross-flow indirect evaporative coolers in general and regenerative operation modes", *Applied Energy*, Vol. 195, pp. 268–277.
Velasco Gómez E., Tejero González A., and Rey Martínez FJ. (2012) "Experimental characterisation of an indirect evaporative cooling prototype in two operating modes", *Applied Energy*, Vol. 97, pp. 340–346.
Tejero-gonzález A., Andrés-chicote M., Velasco-gómez E., and Rey-martínez FJ. (2013) "Influence of constructive parameters on the performance of two indirect evaporative cooler prototypes", *Applied Thermal Engineering*, Vol. 51, pp. 1017–1025.
Chen Y., Yang H., and Luo Y. (2016) "Indirect evaporative cooler considering condensation from primary air: model development and parameter analysis", *Building and Environment*, Vol. 95, pp. 330-345.
Chen Y., Yang H., and Luo Y. (2016) "Parameter sensitivity analysis and configuration optimization of Indirect Evaporative Cooler (IEC) considering condensation", *Applied Energy*, Vol. 104, pp. 87–104.
W. Y. Saman and S. Alizsdeh. (2001) "Modeling and performance analysis of a cross-flow type plate heat exchanger for dehumidification/cooling", *Solar Energy*, Vol. 70 (4), pp. 361–372.

ACKNOWLEDGEMENT

This work was supported by the Korea Agency for Infrastructure Technology Advancement (KAIA) grant (17CTAP-C116268-02), and the Korea Institute of Energy Technology Evaluation and Planning (KETEP) (No. 20164010200860).